

# Cytosine Deaminase APOBEC3A Sensitizes Leukemia Cells to Inhibition of the DNA Replication Checkpoint

Abby M. Green<sup>1,2</sup>, Konstantin Budagyan<sup>3</sup>, Katharina E. Hayer<sup>2,4</sup>, Morgann A. Reed<sup>3</sup>, Milan R. Savani<sup>5</sup>, Gerald B. Wertheim<sup>2,3</sup>, and Matthew D. Weitzman<sup>1,2,3</sup>



## Abstract

Mutational signatures in cancer genomes have implicated the APOBEC3 cytosine deaminases in oncogenesis, possibly offering a therapeutic vulnerability. Elevated APOBEC3B expression has been detected in solid tumors, but expression of APOBEC3A (A3A) in cancer has not been described to date. Here, we report that A3A is highly expressed in subsets of pediatric and adult acute myelogenous leukemia (AML). We modeled A3A expression in the THP1 AML cell line by introducing an inducible A3A gene. A3A expression caused ATR-dependent phosphorylation of Chk1 and cell-cycle arrest, consistent with replication

checkpoint activation. Further, replication checkpoint blockade via small-molecule inhibition of ATR kinase in cells expressing A3A led to apoptosis and cell death. Although DNA damage checkpoints are broadly activated in response to A3A activity, synthetic lethality was specific to ATR signaling via Chk1 and did not occur with ATM inhibition. Our findings identify elevation of A3A expression in AML cells, enabling apoptotic sensitivity to inhibitors of the DNA replication checkpoint and suggesting it as a candidate biomarker for ATR inhibitor therapy. *Cancer Res*; 77(17): 4579–88. ©2017 AACR.

## Introduction

Mutational signatures in cancer genomes have elucidated potential etiologies of DNA damage and oncogenesis (1, 2). Possible mutagens include both endogenous and exogenous sources. One mutational signature, which consists of clustered cytosine mutations and predominantly C→T transitions within a TC context, has been attributed to the APOBEC3 (A3) family of DNA cytosine deaminases. A3 enzymes are best defined by their ability to mutate viral DNA and restrict infection, although the full scope of their endogenous function is unknown (3). Two A3 family members, A3A and A3B, are localized in the nucleus (4) and their activity results in cellular DNA damage (5–7). A3 enzymes are postulated to be under tight regulation to prevent detrimental genotoxicity.

The association between A3 family members and cancer mutagenesis has emerged through identification of the A3 mutational signature in cancer genomes, as well as increased A3 expression in human tumors. Most notably, several studies have detected elevated A3B expression correlated with mutational hallmarks in breast cancer (7, 8). The related A3A has also been implicated in mutational signatures identified in cancer genomes (9, 10). The mutational signatures of A3A and A3B are similar but distinguishable and that of A3A is the more prominent signature in cancer genomes (9). A germline polymorphism that deletes the A3B coding sequence and fuses A3A to the 3'UTR of A3B has been associated with increased stability of A3A transcripts, a higher burden of A3 mutational signatures, and cancer susceptibility (11–13). Despite these strong associations between A3A and mutational burden in cancer genomes, A3A expression in human cancers has not been established.

Endogenous expression of A3 enzymes is largely restricted to immune tissues, although variations exist across A3 family members (14). A3A is highly expressed in myeloid lineage cells and is interferon-inducible in lymphocytes (15–17). Although A3A expression in peripheral blood mononuclear cells represents the highest level of endogenous expression of any A3 family member in human tissue (14), A3A expression in hematologic malignancies has not been investigated.

A3A expression results in robust activation of cellular DNA damage responses (5, 6). Ectopic A3A expression has been shown to cause phosphorylation of histone variant H2AX and ATM (Ataxia-Telangiectasia Mutated) kinase, indicative of a cellular response to double-stranded DNA breaks (DSB; ref. 6). We recently showed that A3A expression also causes replication stress, as evidenced by activation of ATR (ATM- and Rad3-related) kinase, phosphorylation of downstream Chk1 (Checkpoint Kinase 1), and cell-cycle arrest (5). The ATR-Chk1

<sup>1</sup>Department of Pediatrics, Children's Hospital of Philadelphia and University of Pennsylvania Perelman School of Medicine, Philadelphia, Pennsylvania. <sup>2</sup>Center for Childhood Cancer Research, Children's Hospital of Philadelphia, Philadelphia, Pennsylvania. <sup>3</sup>Department of Pathology and Laboratory Medicine, Children's Hospital of Philadelphia and University of Pennsylvania Perelman School of Medicine, Philadelphia, Pennsylvania. <sup>4</sup>Department of Biomedical and Health Informatics, Children's Hospital of Philadelphia, Philadelphia, Pennsylvania. <sup>5</sup>University of Pennsylvania College of Arts and Sciences, Philadelphia, Pennsylvania.

**Note:** Supplementary data for this article are available at Cancer Research Online (<http://cancerres.aacrjournals.org/>).

A.M. Green and K. Budagyan contributed equally to the article.

**Corresponding Author:** Matthew D. Weitzman, The Children's Hospital of Philadelphia, 3501 Civic Center Boulevard, Philadelphia, PA 19104. Phone: 267-425-2068; Fax: 267-426-2791; E-mail: weitzmanm@email.chop.edu

**doi:** 10.1158/0008-5472.CAN-16-3394

©2017 American Association for Cancer Research.

pathway is activated in response to replication stress when Replication Protein A (RPA) binds exposed ssDNA and recruits ATR localization and activation (18). ATR signaling promotes replication fork stability and enforces the replication checkpoint that arrests cellular division to allow for repair of damaged DNA before mitosis (19). Inhibition of the replication checkpoint promotes replication fork collapse into DSBs and genotoxicity, particularly in the context of DNA damage that impedes DNA polymerase progression. These conditions can be cancer-associated, including the effects of oncogene expression (20, 21). Thus, the ATR–Chk1 pathway has been investigated as a target for cancer therapy (22, 23).

Effective cancer therapy relies on differences between healthy cells and cancer cells that present opportunities for selective targeting. Traditional chemotherapeutics target fundamental cellular processes, such as DNA replication, which results in death of rapidly dividing cancer cells but have a high level of toxicity in proliferating healthy cells. One potential for more refined therapies occurs in the context of synthetic lethality, in which two abnormal gene products cooperate to impair cell fitness more than either one alone (24). Synthetic lethality can be prompted by drug-induced inhibition of essential pathways in genetically altered cancer cells. Here, we investigate the hypothesis that inhibition of genome-protective DNA damage responses enables A3A-induced genotoxicity and can result in synthetic lethality.

In this study, we show that A3A expression is elevated in subsets of human acute myelogenous leukemia (AML). Our findings present the first demonstration of elevated A3A expression in human cancer, and the first association of A3 enzymes with hematologic malignancies. To model the effects of high A3A expression, we developed an AML cell line with inducible A3A expression. We demonstrate that the DNA replication checkpoint is robustly activated by A3A in leukemia cells and that A3A sensitizes AML cells to treatment with small-molecule inhibitors of ATR and Chk1 kinases. We determined that A3A deamination renders cancer cells dependent on the replication checkpoint for genome protection and that this can be exploited to induce synthetic lethality. Taken together, our data contribute to a new, targeted treatment paradigm for human cancers with elevated A3A expression.

## Materials and Methods

### Cell lines

Authenticated THP1, K562, CEM, Ramos, and U2OS cells were purchased from the ATCC. U937 cells were a kind gift from Sarah Tasian. Cell lines were not further authenticated. All cells were obtained within 5 years before use in experiments described. Cells were tested and confirmed to be mycoplasma free. All cell lines were maintained in RPMI containing 100 U/mL of penicillin and 100 µg/mL of streptomycin, and supplemented with 10% tetracycline-free FBS. Cells were used within 8 weeks of thawing for experiments described. To construct inducible A3A cell lines, HA-tagged A3A cDNAs were inserted into an entry vector with the CMV promoter and upstream Tetracycline Response Element (pEN\_Tmcs). Cloning primer sequences are available upon request. A pSLIK-A3A plasmid was generated by Gateway cloning of the pEN\_Tmcs-A3A plasmid into a pSLIK lentivirus vector with a constitutively expressed neomycin resistance gene and tetracycline transactivator (25) to generate a single

vector system of doxycycline-inducible expression of A3A-HA. Production of lentiviral particles was achieved by transfection of 293T cells as described previously (26). Following transduction with the pSLIK-A3A lentivirus, cells were selected in 1 mg/mL neomycin. After selection, cells were maintained in 0.5 mg/mL neomycin. Knockdown of endogenous A3A in U937 cells was achieved by stable expression of short hairpin RNA against A3A (shA3A). Lentivirus vectors (pLKO) containing shA3A and shControl were purchased from Sigma. Production of lentivirus was achieved as above, and following transduction with the pLKO-shRNA lentivirus, cells were selected in 1 µg/mL puromycin. All cells were grown at 37°C in a humidified atmosphere containing 5% CO<sub>2</sub>.

### Small-molecule inhibitors

The ATR kinase inhibitor VE-822 (Vertex), Chk1 kinase inhibitor PF-477736 (Pfizer), and ATM kinase inhibitor KU5933 (Abcam) were each dissolved in dimethyl sulfoxide (DMSO) to make a stock solution and stored at –20°C. Solutions were further diluted in DMSO for treatment of cells in culture. Controls were treated with an equal volume of vehicle (DMSO).

### Cell-cycle analysis

THP1, K562, CEM, and Ramos cells were grown in the presence or absence of doxycycline (1 µg/mL, Clontech), fixed in 70% ice-cold ethanol, washed in PBS, and resuspended in staining solution containing 20 mg/mL propidium iodide (Sigma) and 200 mg/mL RNase A (Roche). Data were collected using an Accuri C6 Flow Cytometer (BD Biosciences) and analyzed by FlowJo software (Version 10.2). Experiments were each performed three times, and at least 20,000 cells were analyzed per sample.

### Immunoblotting and immunofluorescence

For immunoblotting, lysates were prepared by harvesting cells in 10% SDS sample buffer (Novex) and 5% β-mercaptoethanol (Sigma) and boiling for 10 minutes, then run on Bis-Tris gels and transferred to a polyvinylidene fluoride membrane (PVDF, Amersham). For immunofluorescence, cells were fixed with 4% paraformaldehyde and permeabilized with 0.5% Triton X-100 for 10 minutes. Nuclei were visualized by staining with 4,6-diamidino-2-phenylindole (DAPI, Sigma). Images were acquired using a Zeiss LSM 710 confocal microscope. Quantification of cell staining was performed on at least 50 cells per condition. Representative images are shown.

### Antibodies

Commercially available antibodies used in this study were obtained from Cell Signaling Technology (Chk2-p-T68, Chk1-p-S345, Chk1-p-S317), Millipore (Chk2), Epitomics (ATM), Abcam (ATM-p-S1981), Santa Cruz Biotechnology (Chk1, Actin), Bethyl Laboratories (RPA32), GeneTex (GAPDH), Biolegend (HA), and the NIH AIDS Reagent Program (A3A/A3G C-terminal polyclonal antibody). Secondary antibodies for immunoblotting included goat anti-rabbit IgG and goat anti-mouse IgG (Jackson ImmunoResearch).

### Proliferation, viability, and apoptosis assays

**Proliferation assay.** Leukemia cells were plated at density of 1,000 to 5,000 cells per well in a 96-well plate. Cells were precultured for 24 hours, then treated with doxycycline (1 µg/mL) and a range of small-molecule inhibitor doses or vehicle control (DMSO).

Cells were then cultured for 48 hours. Water-soluble tetrazolium salt reagent (CCK-8, Dojindo) was added 2 to 4 hours before analysis. Data were collected using an Infinity M1000 Pro plate reader (Tecan).

**Viability assay.** Leukemia cells were plated at density of 300,000 cells per well in a 6-well plate. Cells were treated with doxycycline (1  $\mu\text{g}/\text{mL}$ ) and small-molecule inhibitor or vehicle control for 48 hours. Cells were stained using the Live/Dead Kit (Invitrogen) according to the manufacturer's instructions. Data were collected using an Accuri C6 Flow Cytometer (BD Biosciences).

**Apoptosis assay.** Leukemia cells were plated at density of 300,000 cells per well in a 6-well plate. Cells were treated with doxycycline (0.1  $\mu\text{g}/\text{mL}$ ) and small-molecule inhibitor or vehicle control. Cells were cultured for 48 hours following treatment and then stained using FITC Annexin-V Kit (BD Biosciences) according to the manufacturer's instructions.

#### RNA isolation, cDNA synthesis, and qPCR

Primary AML samples were obtained from the University of Pennsylvania Stem Cell and Xenograft Core. RNA was extracted from primary samples and cell lines using the RNeasy Minikit (Qiagen). cDNA was made using the High Capacity RNA to cDNA Kit (Applied Biosystems). Quantitative PCR (qPCR) was performed with SYBR Green PCR Master Mix (Applied Biosystems) on a ViiA 7 real-time PCR instrument (Applied Biosystems). Primers were designed to distinguish A3A from A3B and are as follows: A3A forward, CACAACCAGGCTAAGAATCTTCTC; A3A reverse, CAGTGCTTAAATTCATCGTAGGTC; A3B forward, GAA-TCCACAGATCAGAAATCCGA; and A3B reverse, TTTCACITTCATAGCACAGCCA. The housekeeping gene cyclophilin was used for normalization. For comparison of primary AML samples, a pool of all primary samples was used for  $\Delta\Delta C_t$  analysis. For comparison of THP1-A3A to primary AML samples, all samples were normalized to THP1-A3A cells induced with doxycycline for  $\Delta\Delta C_t$  analysis. For comparison of AML cell lines, a pool of all cell lines was used for  $\Delta\Delta C_t$  analysis.

#### Bioinformatic analysis

Primary tumor RNA sequencing data were obtained from public sources. Raw count data for genes expressed in The Cancer Genome Atlas (TCGA)-LAML ( $n = 151$ ) and Therapeutically Applicable Research to Generate Effective Treatments (TARGET)-AML ( $n = 282$ ) were downloaded from the GDC Data Portal. Data were normalized using the bioconductor package DESeq2 (27). The normalized gene expression for A3A was separated into two groups, using the 1.5 times the IQR to determine high-expression outliers (28). The results shown here are based upon data generated by the TCGA Research Network (<http://cancergenome.nih.gov>), and by the Therapeutically Applicable Research to Generate Effective Treatments (TARGET) initiative managed by the NCI (<http://ocg.cancer.gov/programs/target>). The data used for this analysis are available at GDC Data portal (<https://gdc-portal.nci.nih.gov/>).

#### Statistical analysis

To distinguish significant differences between high and low A3A expression groups we applied the Mann-Whitney  $U$  test. Boxplot statistics were computed with the function "boxplot" of R programming language.  $P$  values and SEM for cell-cycle analysis, Annexin V staining, and Live/Dead staining were obtained by

paired two-tailed  $t$  tests.  $P$  values and SEM for proliferation assays were determined by the sum-of-squares  $F$  test. Results were considered significant at  $P < 0.05$ . GraphPad Prism 7 software was used for statistical analysis.

## Results

### A3A is highly expressed in a subset of pediatric and adult AML

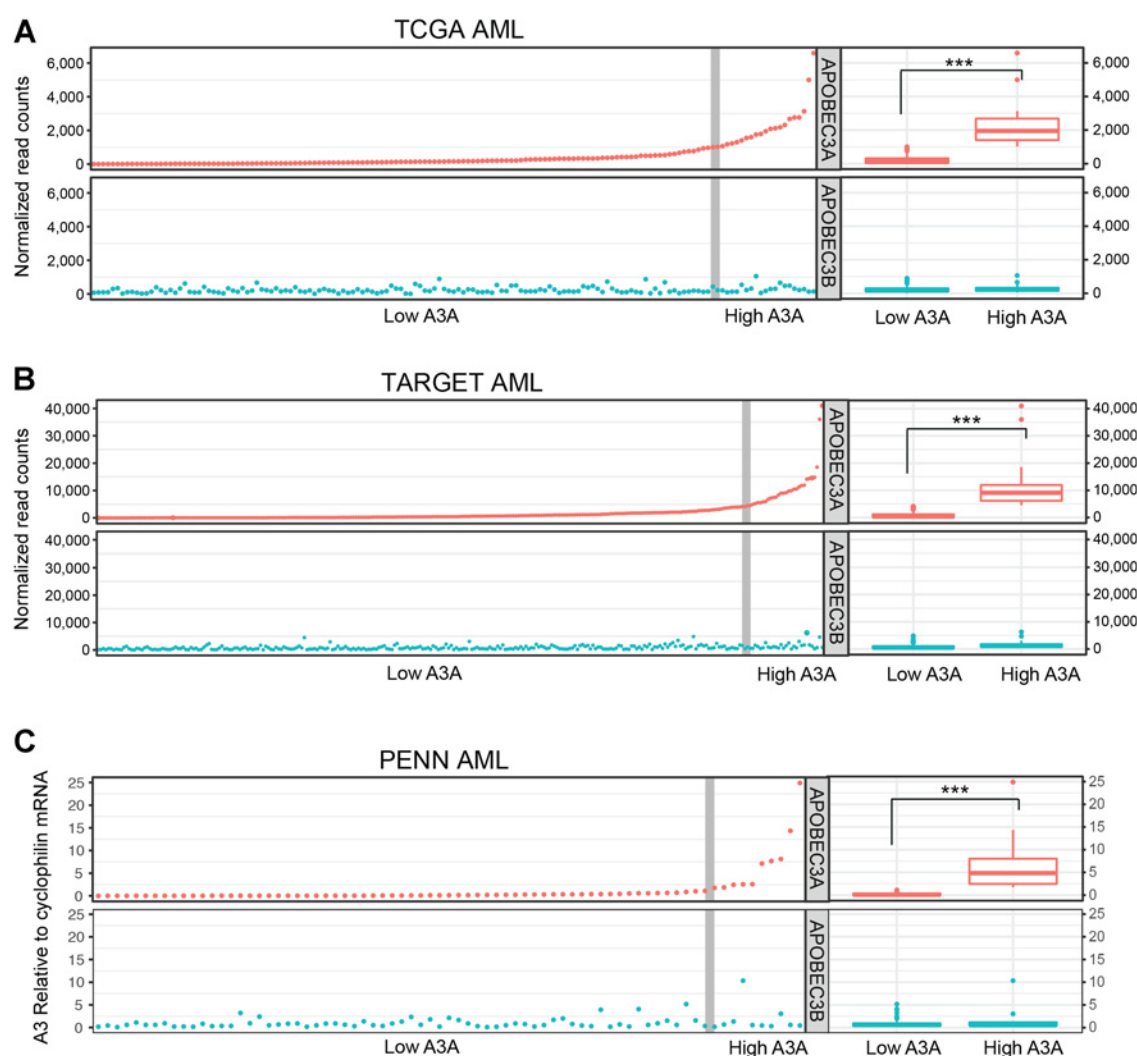
To determine which types of human leukemia are most impacted by A3A activity, we examined RNA-sequencing (RNA-seq) data from two major databases of primary leukemias: TCGA that comprises expression data from adult-onset tumors and TARGET, which includes expression profiles of childhood cancers. We limited our evaluation of A3A expression to samples with RNA-seq data, because microarray probes are insufficient to distinguish specific A3 transcripts given their high degree of homology (7). Analysis of RNA-seq from available data showed that high A3A expression occurs in subsets of both pediatric and adult AML (Fig. 1A and B; Supplementary Table S1). A3A expression levels 1.5 times greater than the interquartile range (IQR) were considered high expression outliers (28). The remaining values were assigned to the low expression group. The high A3A expression group comprised 14% of the TCGA samples and 11% of the TARGET samples. Because A3B is reported to be overexpressed in many human cancers (29), we evaluated expression levels of A3B in the same patient samples (Fig. 1A–B; Supplementary Fig. S1A–S1B). When the high A3A and low A3A groups were analyzed in aggregate, we found no difference in average A3B expression between the groups (Fig. 1A and B). An additional analysis of samples with outlier A3B expression showed that this group did not overlap with samples in the outlier A3A expression group. There were fewer samples with A3B outlier expression (6% of TCGA and 4% of TARGET), and A3B outlier expression was several log-fold lower than the expression of A3A outliers (Supplementary Fig. S1A–S1B).

We obtained primary AML samples from a biorepository at the University of Pennsylvania (PENN) and evaluated A3A mRNA expression by quantitative real-time PCR (qPCR). Consistent with results from TCGA and TARGET datasets, 13.3% of PENN patient samples exhibited high outlier A3A expression (Fig. 1C; Supplementary Table S1). Analysis of high A3A and low A3A groups indicated no difference in average A3B mRNA levels in either group (Fig. 1C). In addition, in primary AML samples, outlier A3B expression did not correlate with elevated A3A expression (Supplementary Fig. S1C). Together, these data indicate that A3A is highly expressed in a subset of pediatric and adult AML.

### The replication checkpoint is activated by A3A in leukemia cells

We previously showed that replicating cells are more susceptible to DNA damage by A3A than quiescent cells (5), likely due to deamination of single-stranded DNA (ssDNA) substrate at replication forks (30, 31). We sought to evaluate whether this process occurs in leukemia cells in which A3A is active. We constructed a model AML cell line (THP1) with a doxycycline-inducible HA-tagged A3A gene, in which titration of doxycycline dosing enables control of A3A expression levels. In our inducible THP1-A3A cell line, treatment with 1  $\mu\text{g}/\text{mL}$  doxycycline resulted in A3A expression similar to that of primary AML samples from

Green et al.

**Figure 1.**

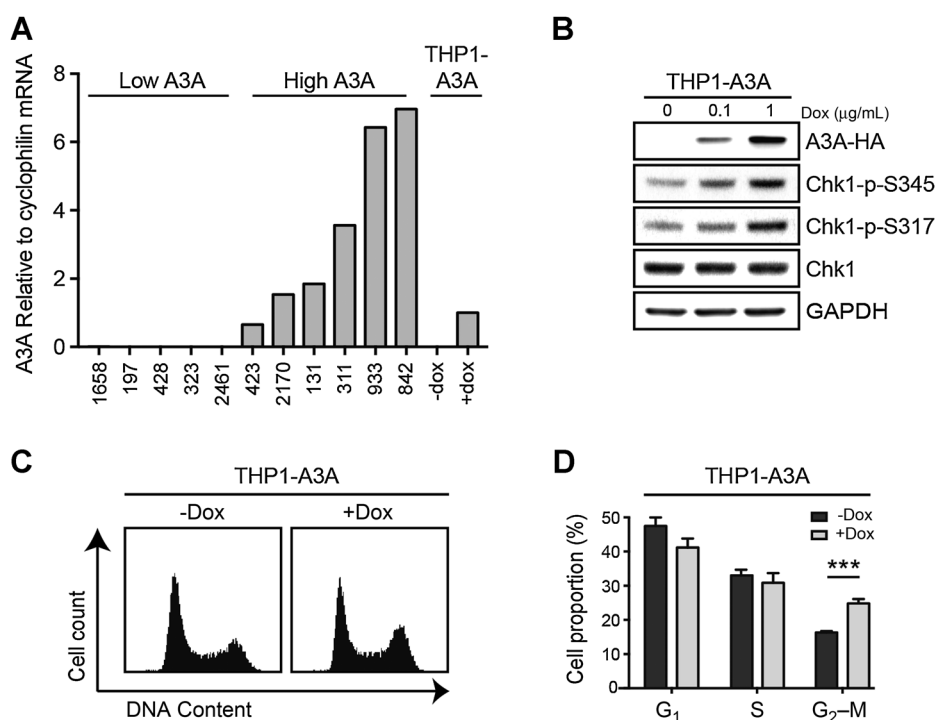
APOBEC3A is highly expressed in AML. APOBEC3A (red) and APOBEC3B (blue) expression was evaluated in three large cohorts of primary AML. A3 expression in AML samples from the TCGA (A) and TARGET (B) databases was determined by RNA-sequencing analysis. Evaluation of A3 mRNA levels in primary AML samples from the University of Pennsylvania (PENN) biological repository (C) was performed by quantitative PCR; A3 mRNA level is displayed as fold change relative to a pooled control. Scatter plots (left) show normalized expression of A3A and A3B in individual samples. Vertical gray line denotes a subset of high A3A expression outliers (right) determined by  $1.5 \times$  interquartile range. Box plots (far right) display aggregate expression of A3A and A3B in high A3A and low A3A groups. Statistical analysis was performed using the Mann-Whitney *U* test. \*\*\*,  $P \leq 0.001$ .

PENN categorized as having high A3A expression (Fig. 2A). We examined checkpoint activation by immunoblotting with phospho-specific antibodies that recognize sites attributable to ATR kinase activity. We observed a dose-response relationship between A3A protein level and Chk1 phosphorylation at serines 317 and 345 (Fig. 2B; ref. 32). To evaluate whether deaminase activity is required for ATR activation, we generated a THP1 cell line with an inducible HA-tagged A3A mutant (C106S) lacking enzymatic activity (15). Immunoblotting showed that when A3A-C106S was induced there was no significant change in phosphorylation of Chk1 at serines 317 and 345 (Supplementary Fig. S2). Thus, the enzymatic activity of A3A appears to be required for replication checkpoint activation. We also show that RPA foci accumulate upon A3A expression, supporting the conclusion that A3A expression results in replication stress and

accumulated ssDNA (Supplementary Fig. S3). We then evaluated THP1 cell-cycle profiles upon A3A induction by propidium iodide staining. A3A induction resulted in  $G_2$  arrest, consistent with replication checkpoint activation (Fig. 2C and D). Similar results were observed in a panel of A3A-inducible leukemia cell lines representative of chronic myelogenous leukemia (K562), acute T-lymphoblastic leukemia (CEM), and B-lymphoblastic leukemia (Burkitt, Ramos; Supplementary Fig. S4A-S4C). These data indicate that A3A deamination results in replication checkpoint activation in hematopoietic cells.

#### A3A sensitizes AML cells to ATR inhibition

Because A3A activates the replication checkpoint, we hypothesized that inhibition of checkpoint signaling would result in genotoxicity in AML cells with high A3A expression. We

**Figure 2.**

APOBEC3A expression results in ATR activation and checkpoint arrest in AML cells. The AML cell line, THP1, was generated to express A3A upon treatment with doxycycline. **A**, Expression levels of A3A in inducible THP1 cells are similar to those of primary AML samples with high A3A expression. Evaluation of A3A mRNA levels was performed by qPCR in THP1-A3A cells treated with doxycycline (Dox; 1 µg/mL) alongside primary AML samples from the PENN dataset. Primary AML samples included a selection of those with high A3A and low A3A expression. A3A expression level is displayed as fold change relative to doxycycline-treated THP1-A3A cells. **B**, ATR signaling is activated by A3A expression. Cells were treated with indicated concentrations of doxycycline and analyzed by immunoblotting using antibodies to HA, Chk1, and phosphorylated Chk1 (S345 and S317). GAPDH was used as a loading control. **C**, A3A expression results in G<sub>2</sub> arrest. Inducible cells were treated with doxycycline (1 µg/mL) for 48 hours and analyzed for cell-cycle progression by propidium iodide staining. **D**, Accompanying chart shows fraction of cells in G<sub>1</sub>, S, and G<sub>2</sub> phase pre- and post-induction; error bars, SEM. Statistical analysis was performed using a paired two-tailed *t* test. Results are representative of three independent replicates. \*\*\*, *P* ≤ 0.001.

therefore treated the THP1-A3A AML cell line with the ATR kinase inhibitor VE-822 (ATRi), a potent and specific drug that is currently being evaluated in clinical trials in combination with chemotherapy for refractory solid tumors (33–35). We examined the impact of ATR inhibition in our THP1-A3A cells by inducing A3A and then treating with a range of doses of ATRi. THP1 cells that were induced to express A3A had significantly decreased viability after treatment with ATRi when compared with uninduced cells (Fig. 3A, left). Notably, A3A induction resulted in an impressive shift of the ATRi half maximal effective concentration (EC<sub>50</sub>) from 5,700 nmol/L to 150 nmol/L. Immunoblotting showed decreased phosphorylation of Chk1 in cells treated with ATRi, confirming inhibition of ATR activity (Fig. 3A, right).

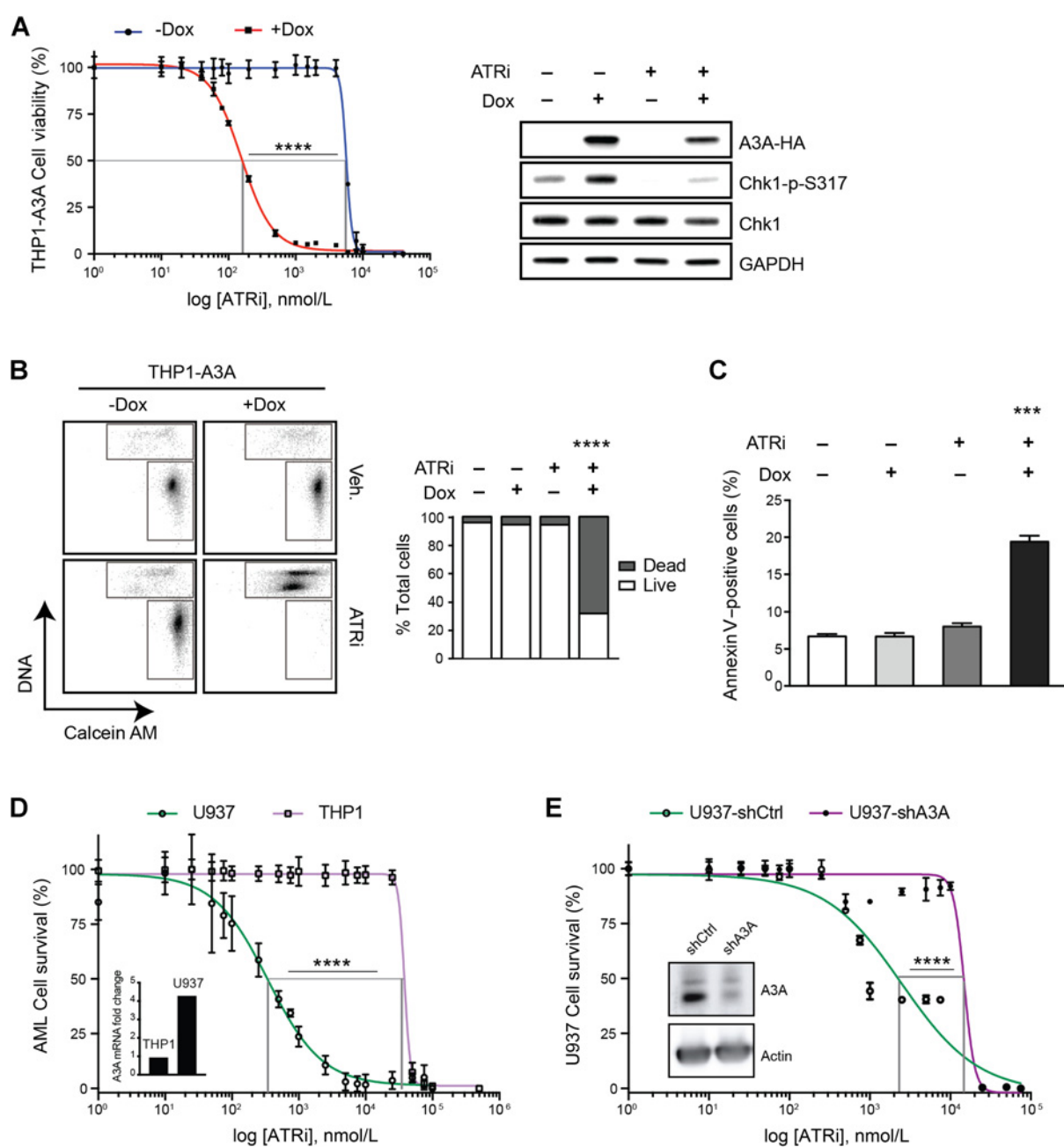
We further assessed cytotoxicity of ATRi treatment in THP1-A3A cells using a DNA stain and a fluorescent-labeled cell membrane stain (calcein AM) that permeates intact cells. Flow cytometric analysis showed a significant increase in the fraction of dead cells when A3A expression was combined with low-dose ATRi as compared with controls (Fig. 3B). In addition, we found increased Annexin V staining in cells treated with both doxycycline and ATRi, suggesting that cell death occurs by apoptosis (Fig. 3C). Together, these findings indicate that A3A expression sensitizes AML cells to treatment with a selective ATR inhibitor.

To determine the contribution of endogenous A3A to sensitivity of AML cells by ATR inhibition, we used two approaches. First, we evaluated expression of A3A in AML cell lines and found that the U937 cell line had relatively high A3A expression compared to THP1 (Fig. 3D, inset). We assessed viability of these cell lines after treatment with ATRi and found that U937 cells were more susceptible to ATRi treatment than THP1 (Fig. 3D). Second, we knocked down endogenous A3A in U937 cells using short hairpin RNA against A3A (shA3A). By immunoblotting, we show that A3A expression is decreased in cells with stable expression of shA3A compared with a control shRNA (Fig. 3E, inset). We treated U937-shA3A and U937-shCtrl cells with ATRi and observed decreased viability in cells with higher A3A expression (Fig. 3E). Thus, high endogenous A3A expression correlates with increased sensitivity of AML cell lines to ATRi treatment.

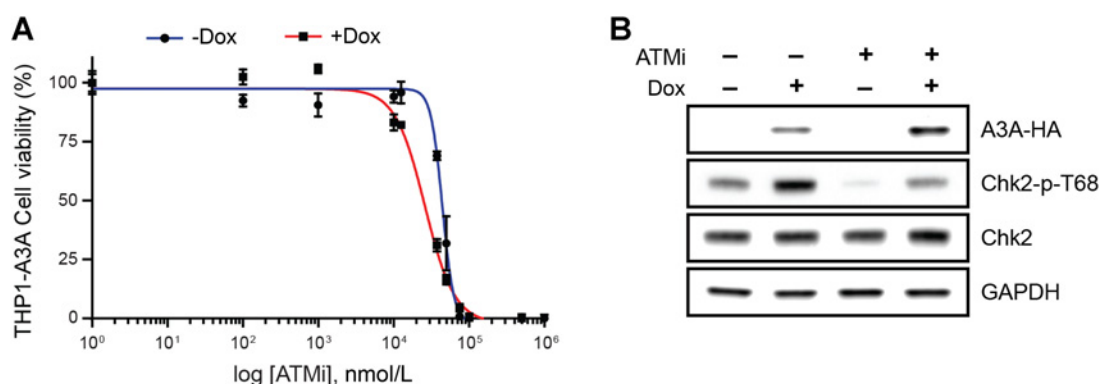
#### Synthetic lethality with high A3A expression is specific to the ATR–Chk1 pathway

We previously showed that A3A activates parallel arms of the DNA damage response via both ATM and ATR kinases (5, 6). On the basis of the finding that A3A sensitizes leukemia cells to ATRi, we hypothesized that an ATM inhibitor (ATMi) would also result in synthetic lethality. We tested this hypothesis by treating the THP1-A3A cell line with a specific ATMi

Green et al.

**Figure 3.**

APOBEC3A sensitizes AML cells to ATR inhibition. **A**, A3A expression was induced in THP1-A3A cells by addition of doxycycline (Dox; 1  $\mu$ g/mL) and then treated with indicated doses of a small-molecule inhibitor of ATR kinase (ATRi, VE-822) 48 hours before analysis. Viability was determined by colorimetric change after addition of a water-soluble tetrazolium salt. Statistical analysis of  $EC_{50}$  was performed using a sum-of-squares F-test. Error bars, SEM. Accompanying immunoblot shows impact of ATRi treatment on THP1-A3A cells treated with doxycycline, ATRi (80 nmol/L), or combinations. Cell lysates were probed with antibodies to HA, Chk1, and phosphorylated Chk1. GAPDH was used as loading control. **B**, THP1-A3A cells were treated with doxycycline (1  $\mu$ g/mL), ATRi (200 nmol/L), or combinations, incubated with fluorescent-labeled calcein AM (live) and DNA (dead) stains, then evaluated by FACS. The upper gate includes dead cells and the lower gate includes live cells. Accompanying bar chart shows quantitation of results averaged over three replicates. Statistical analysis was performed using a paired two-tailed *t* test; error bars, SEM. **C**, THP1-A3A cells were treated with 0.1  $\mu$ g/mL doxycycline, ATRi (80 nmol/L), or combinations. Apoptosis was evaluated by FACS analysis after Annexin V staining and results are displayed as quantitation of three replicate experiments. Statistical analysis was performed using a paired two-tailed *t* test; error bars, SEM. **D**, Endogenous A3A expression was evaluated by qPCR in the U937 and THP1 AML cell lines (inset). A3A level is shown as fold-change relative to a pooled control sample. AML cell lines were treated with indicated doses of ATRi for 48 hours before analysis of cell viability. **E**, shRNA was used to deplete endogenous A3A in the U937 AML cell line. Cells transduced with lentivirus containing control (U937-shCtrl) and A3A (U937-shA3A) shRNAs were evaluated by immunoblot using an antibody to endogenous A3A (inset). Actin was used as a loading control. U937 cells were treated with indicated doses of ATRi for 48 hours before analysis of cell viability. Statistical analysis of  $EC_{50}$  was performed using a sum-of-squares F-test; error bars, SEM. \*\*\*,  $P \leq 0.001$ , \*\*\*\*,  $P \leq 0.0001$ .

**Figure 4.**

APOBEC3A does not sensitize leukemia to ATM inhibition. THP1-A3A cells were treated with doxycycline (Dox; 1  $\mu\text{g}/\text{mL}$ ) to induce A3A expression and a small-molecule inhibitor of ATM kinase (ATMi, KU55933). **A**, Viability was determined by colorimetric change after incubation with a water-soluble tetrazolium salt. Statistical analysis was performed using a sum-of-squares F-test; error bars, SEM. **B**, Inhibition of ATM activity was analyzed by immunoblot of THP1-A3A cell lysates treated with doxycycline (1  $\mu\text{g}/\text{mL}$ ), ATMi (10  $\mu\text{mol}/\text{L}$ ), and combination. Antibodies to HA, Chk2, and phosphorylated Chk2 (T68) were used. GAPDH was used as a loading control.

(KU55933; ref. 36) but found no difference in viability of induced and uninduced cells (Fig. 4A). Immunoblotting confirmed that ATMi efficiently decreased Chk2 phosphorylation, and therefore blocked ATM activity (Fig. 4B). To strengthen this finding, we used two cell models of inducible A3A expression with genetic abrogation of ATM. First, we knocked down ATM expression by siRNA in a U2OS-A3A cell line. A3A expression resulted in phosphorylation of ATM and Chk2, which was effectively inhibited by siRNA knock-down of ATM (Supplementary Fig. S5A, right). However, we observed that ATM knockdown had no effect on cell viability (Supplementary Fig. S5A, left). Second, we examined immortalized human fibroblasts derived from a patient with Ataxia-Telangiectasia that express nonfunctional ATM (-ATM), and compared with isogenic cells complemented with wild-type ATM (+ATM; ref. 37). When ectopic A3A was expressed in both cell lines, no difference in viability was observed (Supplementary Fig. S5B). Together, these data show that A3A activity does not sensitize cells to ATM inhibition.

We hypothesized that the ATR-Chk1 function in cell-cycle checkpoint activation is central to susceptibility of cells with high A3A expression. Checkpoint activation occurs through ATR phosphorylation of the downstream effector Chk1 (38). We examined cell-cycle profiles in THP1-A3A cells expressing A3A in the presence of either ATRi or a small-molecule Chk1 inhibitor (Chk1i, PF477736; refs. 39, 40). Upon A3A induction, cell-cycle profiles of THP1 cells showed an arrest in G<sub>2</sub>, which returned to baseline after treatment with either ATRi or Chk1i (Fig. 5A; Supplementary Fig. S6A–6B). Thus, inhibition of the ATR–Chk1 pathway abrogates A3A-induced cell-cycle arrest. We then examined the susceptibility of THP1-A3A cells to Chk1i. Treatment with Chk1i led to decreased viability and cell death when A3A was expressed (Fig. 5B and C). Chk1i exhibited a very large therapeutic index with a shift in EC<sub>50</sub> from 250,000 to 66 nmol/L upon A3A induction. Inhibition of Chk1 activity by PF477736 was confirmed by diminished phosphorylation of Chk1 at serine 296 (Fig. 5B, right; ref. 41). These data show that the ATR–Chk1 checkpoint function is activated by A3A-induced replication stress and that abrogation of checkpoint activation leads to death of leukemia cells.

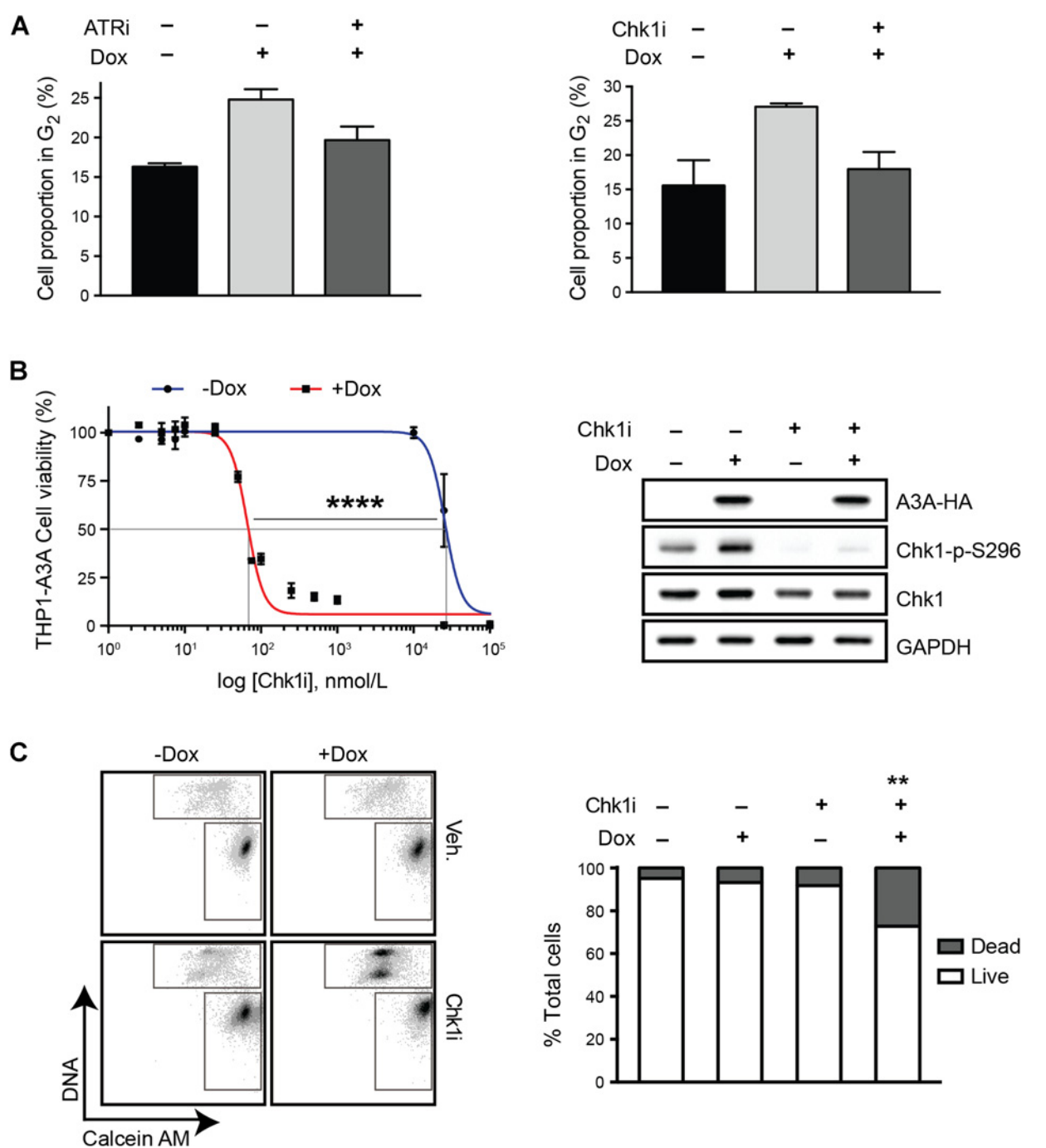
## Discussion

Emerging data provide compelling evidence that APOBEC3 enzymes act on the cellular genome. Increased expression of A3 family members has been detected in several types of human cancer (29) and A3 mutational signatures have been discovered in tumor genomes (1, 2, 8). Mutational burden associated with A3 activity has led to speculation about their oncogenic potential (7), influence on clonal evolution of cancer cells, and contribution to treatment resistance and aggressive phenotypes (42). In this study, we investigate an alternative outcome of the interaction of A3 enzymes with cancer genomes in which A3 activity can be exploited for targeted cancer therapy.

APOBEC3 enzymes are proposed sources of both clustered and dispersed cytidine mutations in cancer genomes (1, 9, 31). Clustered mutations, termed kataegis, are postulated to occur due to A3 mutagenesis of ssDNA generated by resection of ends at DNA breakpoints. Discontinuous synthesis at the lagging strand during replication likely provides substrate for dispersed patterns of cytosine deamination by A3 (30, 31, 43). We recently showed that replicating cells incur more DNA damage caused by A3A when compared with nonreplicating cells (5). These data point to a model of A3 deamination at replication forks, which suggests that frequently replicating cells are particularly susceptible to damage by A3 enzymes. Consistent with this model, the replication checkpoint, regulated by ATR–Chk1 signaling, is activated in response to A3A expression. Our data suggest that A3A expression results in increased ssDNA accumulation, likely due to stalling of replicative polymerases at uracil lesions or abasic sites, providing further substrate for A3A activity. If unchecked, A3A deamination may result in increasing levels of mutagenesis, irreversible genome damage, and cytotoxicity. In support of this model, we find that cells with high A3A expression are dependent on the ATR–Chk1 checkpoint for survival, and inhibition of this pathway results in cell death.

Previous studies have shown broad DNA damage responses to A3A expression, including phosphorylation of histone

Green et al.

**Figure 5.**

Sensitization to ATR inhibition by A3A is dependent on the ATR checkpoint function. THP1-A3A cells were treated with 1  $\mu\text{g}/\text{mL}$  doxycycline (Dox) to induce A3A expression, and a small-molecule inhibitor of ATR or Chk1 kinase before analysis. **A**, Checkpoint arrest is abrogated by a small-molecule inhibition of ATR or Chk1. THP1-A3A cells were treated with doxycycline for 48 hours and analyzed for cell-cycle progression by propidium iodide staining. Accompanying chart shows fraction of cells in  $G_2$  phase before doxycycline induction, after doxycycline induction, and after doxycycline induction combined with kinase inhibitor (80 nmol/L ATRi or 30 nmol/L Chk1i) treatment. Statistical analysis was performed using a paired two-tailed *t* test; error bars, SEM. **B**, Viability of THP1-A3A cells was measured after treatment with indicated doses of Chk1i. Cell viability was determined by metabolism of a water-soluble tetrazolium salt. Statistical analysis of  $EC_{50}$  was performed using a sum-of-squares F-test. Error bars, SEM. Immunoblotting shows inhibition of Chk1 kinase activity upon treatment with Chk1i (30 nmol/L), indicated by decreased phosphorylation of Chk1 at serine 296. Antibodies to HA, Chk1, and phosphorylated Chk1 (S296) were used. GAPDH was used as a loading control. **C**, Cell death was measured by staining THP1-A3A cells with fluorescently labeled calcein AM (live) and DNA (dead) stains after treatment with doxycycline (1  $\mu\text{g}/\text{mL}$ ), Chk1i (100 nmol/L), or combinations. The upper gate on the FACS plot includes dead cells and the lower gate includes live cells. Accompanying bar chart shows quantitation of FACS results averaged over three replicates. Statistical analysis was performed using a paired two-tailed *t* test; error bars, SEM. \*\*,  $P \leq 0.01$ ; \*\*\*\*,  $P \leq 0.0001$ .



variant H2AX and activation of ATM–Chk2 signaling, which is indicative of DSBs (6, 44). In our model system, we also demonstrate ATM–Chk2 activation by A3A, yet in contrast with the ATR–Chk1 axis, inhibition of ATM does not induce cell death. These findings suggest that the essential genome protective mechanism during A3A mutagenesis is a response to replication stress, and not to DSBs. A possible explanation for this conclusion is that ATR is first activated by extensive deamination at replication forks, resulting in overwhelming replication stress and fork collapse, which secondarily leads to DSBs and subsequent ATM signaling. This model of a feed-forward loop, during which A3A activity causes stalled replication leading to increased ssDNA substrate and further deamination, was recently proposed by Buisson and colleagues (45).

Rapidly dividing cancer cells, such as AML blasts, are dependent on the replication checkpoint to maintain genome integrity. Accordingly, replication checkpoint inhibitors (RCi) are being investigated in clinical trials for their activity as chemotherapy sensitizers (35, 46, 47). These RCi approaches are attractive therapeutic options due to limited toxicity in healthy tissues, wide therapeutic window, and efficacy in a broad array of cancers (48). Few studies have addressed the potential for checkpoint inhibition as a therapeutic option in hematologic malignancies. *In vitro* data have shown efficacy for ATRi in killing hematopoietic tumor cell lines with excessive oncogene-induced replication stress, ATM deficiency, or in combination with oxidative stressors (21, 49, 50). ATRi is not frequently investigated as monotherapy in cancers without additional DDR defects; however, the efficacy of ATRi was recently reported in a murine model of MLL-rearranged AML (51). Here, we show that the replication checkpoint is activated by A3A in AML cells, and that A3A expression significantly increases the therapeutic index of ATR and Chk1 inhibitors. Thus, A3A could serve as a powerful biomarker for RCi treatment in AML. Further studies are warranted to examine the impact of cell-cycle checkpoint inhibition in other tumors with elevated expression of the A3 family members. Our data

provide a strong rationale for further preclinical investigation of replication checkpoint inhibition in AML with high A3A expression.

### Disclosure of Potential Conflicts of Interest

No potential conflicts of interest were disclosed.

### Authors' Contributions

**Conception and design:** A.M. Green, K. Budagyan, M.D. Weitzman

**Development of methodology:** A.M. Green, M.D. Weitzman

**Acquisition of data (provided animals, acquired and managed patients, provided facilities, etc.):** K. Budagyan, M.R. Savani, G.B. Wertheim

**Analysis and interpretation of data (e.g., statistical analysis, biostatistics, computational analysis):** A.M. Green, K. Budagyan, K.E. Hayer, M.A. Reed, M.D. Weitzman

**Writing, review, and/or revision of the manuscript:** A.M. Green, K. Budagyan, G.B. Wertheim, M.D. Weitzman

**Administrative, technical, or material support (i.e., reporting or organizing data, constructing databases):** M.R. Savani

**Study supervision:** A.M. Green, M.D. Weitzman

### Acknowledgments

We thank members of the Weitzman Laboratory for insightful discussions and input. We thank Daphne Avgousti, Mateusz Kopyra, and Rahul Sood for technical assistance. We are grateful to Sarah Tasian and Kristina Cole for generously sharing reagents. We thank Rahul Kohli and Eric Brown for critical reading of the article.

### Grant Support

A.M. Green was supported by a Young Investigator Award from the Alex's Lemonade Stand Foundation, and by the NIH (K12 CA076931 and K08 CA212299). Research on APOBEC enzymes in the Weitzman laboratory was supported by grants to M.D. Weitzman from the NIH (CA181259 and CA185799) and funds from The Children's Hospital of Philadelphia.

The costs of publication of this article were defrayed in part by the payment of page charges. This article must therefore be hereby marked *advertisement* in accordance with 18 U.S.C. Section 1734 solely to indicate this fact.

Received December 13, 2016; revised March 18, 2017; accepted June 22, 2017; published OnlineFirst June 27, 2017.

### References

- Nik-Zainal S, Alexandrov LB, Wedge DC, Van Loo P, Greenman CD, Raine K, et al. Mutational processes molding the genomes of 21 breast cancers. *Cell* 2012;149:979–93.
- Alexandrov LB, Nik-Zainal S, Wedge DC, Aparicio SA, Behjati S, Biankin AV, et al. Signatures of mutational processes in human cancer. *Nature* 2013; 500:415–21.
- Harris RS, Dudley JP. APOBECs and virus restriction. *Virology* 2015; 479–480:131–45.
- Lackey L, Law EK, Brown WL, Harris RS. Subcellular localization of the APOBEC3 proteins during mitosis and implications for genomic DNA deamination. *Cell Cycle* 2013;12:762–72.
- Green AM, Landry S, Budagyan K, Avgousti DC, Shalhout S, Bhagwat AS, et al. APOBEC3A damages the cellular genome during DNA replication. *Cell Cycle* 2016;15:998–1008.
- Landry S, Narvaiza I, Linfesty DC, Weitzman MD. APOBEC3A can activate the DNA damage response and cause cell-cycle arrest. *EMBO Rep* 2011; 12:444–50.
- Burns MB, Lackey L, Carpenter MA, Rathore A, Land AM, Leonard B, et al. APOBEC3B is an enzymatic source of mutation in breast cancer. *Nature* 2013;494:366–70.
- Roberts SA, Lawrence MS, Klimczak LJ, Grimm SA, Fargo D, Stojanov P, et al. An APOBEC cytidine deaminase mutagenesis pattern is widespread in human cancers. *Nat Genet* 2013;45: 970–6.
- Chan K, Roberts SA, Klimczak LJ, Sterling JF, Saini N, Malc EP, et al. An APOBEC3A hypermutation signature is distinguishable from the signature of background mutagenesis by APOBEC3B in human cancers. *Nat Genet* 2015;45:1067–72.
- Taylor BJ, Nik-Zainal S, Wu YL, Stebbings LA, Raine K, Campbell PJ, et al. DNA deaminases induce break-associated mutation showers with implication of APOBEC3B and 3A in breast cancer kataegis. *eLife* 2013;2:e00534.
- Xuan D, Li G, Cai Q, Deming-Halverson S, Shrubsole MJ, Shu XO, et al. APOBEC3 deletion polymorphism is associated with breast cancer risk among women of European ancestry. *Carcinogenesis* 2013; 34:2240–3.
- Nik-Zainal S, Wedge DC, Alexandrov LB, Petljak M, Butler AP, Bolli N, et al. Association of a germline copy number polymorphism of APOBEC3A and APOBEC3B with burden of putative APOBEC-dependent mutations in breast cancer. *Nat Genet* 2014;46:487–91.
- Caval V, Suspene R, Shapira M, Vartanian JP, Wain-Hobson S. A prevalent cancer susceptibility APOBEC3A hybrid allele bearing APOBEC3B 3'UTR enhances chromosomal DNA damage. *Nat Commun* 2014;5:5129.
- Refsland EW, Stenglein MD, Shindo K, Albin JS, Brown WL, Harris RS. Quantitative profiling of the full APOBEC3 mRNA repertoire in lymphocytes and tissues: implications for HIV-1 restriction. *Nucleic Acids Res* 2010;38:4274–84.

Green et al.

15. Chen H, Lilley CE, Yu Q, Lee DV, Chou J, Narvaiza I, et al. APOBEC3A is a potent inhibitor of adeno-associated virus and retrotransposons. *Curr Biol* 2006;16:480–5.
16. Peng G, Greenwell-Wild T, Nares S, Jin W, Lei KJ, Rangel ZG, et al. Myeloid differentiation and susceptibility to HIV-1 are linked to APOBEC3 expression. *Blood* 2007;110:393–400.
17. Koning FA, Newman EN, Kim EY, Kunstman KJ, Wolinsky SM, Malim MH. Defining APOBEC3 expression patterns in human tissues and hematopoietic cell subsets. *J Virol* 2009;83:9474–85.
18. Zou L, Liu D, Elledge SJ. Replication protein A-mediated recruitment and activation of Rad17 complexes. *Proc Natl Acad Sci U S A* 2003;100:13827–32.
19. Cimprich KA, Cortez D. ATR: an essential regulator of genome integrity. *Nat Rev Mol Cell Biol* 2008;9:616–27.
20. Gilad O, Nabet BY, Ragland RL, Schoppy DW, Smith KD, Durham AC, et al. Combining ATR suppression with oncogenic Ras synergistically increases genomic instability, causing synthetic lethality or tumorigenesis in a dosage-dependent manner. *Cancer Res* 2010;70:9693–702.
21. Schoppy DW, Ragland RL, Gilad O, Shastri N, Peters AA, Murga M, et al. Oncogenic stress sensitizes murine cancers to hypomorphic suppression of ATR. *J Clin Invest* 2012;122:241–52.
22. Lord CJ, Ashworth A. The DNA damage response and cancer therapy. *Nature* 2012;481:287–94.
23. Puigvert JC, Sanjiv K, Helleday T. Targeting DNA repair, DNA metabolism and replication stress as anti-cancer strategies. *FEBS J* 2016;283:232–45.
24. Kaelin WG Jr. The concept of synthetic lethality in the context of anticancer therapy. *Nat Rev Cancer* 2005;5:689–98.
25. Shin KJ, Wall EA, Zavzavadjian JR, Santat LA, Liu J, Hwang JJ, et al. A single lentiviral vector platform for microRNA-based conditional RNA interference and coordinated transgene expression. *Proc Natl Acad Sci U S A* 2006;103:13759–64.
26. Everett RD, Parsy ML, Orr A. Analysis of the functions of herpes simplex virus type 1 regulatory protein ICP0 that are critical for lytic infection and derepression of quiescent viral genomes. *J Virol* 2009;83:4963–77.
27. Grossman RL, Heath AP, Ferretti V, Varmus HE, Lowy DR, Kibbe WA, et al. Toward a shared vision for cancer genomic data. *N Engl J Med* 2016;375:1109–12.
28. Tukey JW. *Exploratory data analysis*. Reading, MA: Addison-Wesley; 1977. p. 43–44.
29. Burns MB, Temiz NA, Harris RS. Evidence for APOBEC3B mutagenesis in multiple human cancers. *Nat Genet* 2013;45:977–83.
30. Hoopes JI, Cortez LM, Mertz TM, Malc EP, Mieczkowski PA, Roberts SA. APOBEC3A and APOBEC3B preferentially deaminate the lagging strand template during DNA replication. *Cell Rep* 2016;14:1–10.
31. Seplyarskiy VB, Soldatov RA, Popadin KY, Antonarakis SE, Bazykin GA, Nikolaev SI. APOBEC-induced mutations in human cancers are strongly enriched on the lagging DNA strand during replication. *Genome Res* 2016;25:174–182.
32. Zhao H, Piwnicka-Worms H. ATR-mediated checkpoint pathways regulate phosphorylation and activation of human Chk1. *Mol Cell Biol* 2001;21:4129–39.
33. Josse R, Martin SE, Guha R, Ormanoglu P, Pfister TD, Reaper PM, et al. ATR inhibitors VE-821 and VX-970 sensitize cancer cells to topoisomerase I inhibitors by disabling DNA replication initiation and fork elongation responses. *Cancer Res* 2014;74:6968–79.
34. Hall AB, Newsome D, Wang Y, Boucher DM, Eustace B, Gu Y, et al. Potentiation of tumor responses to DNA damaging therapy by the selective ATR inhibitor VX-970. *Oncotarget* 2014;5:5674–85.
35. O’Carrigan B, de Miguel Luken MJ, Papadatos-Pastos D, Brown J, Tunariu N, Perez Lopez R, et al. Phase I trial of a first-in-class ATR inhibitor VX-970 as monotherapy (mono) or in combination (combo) with carboplatin (CP) incorporating pharmacodynamics (PD) studies. *J Clin Oncol* 2016;34:15 s:2504.</bib>
36. Hickson I, Zhao Y, Richardson CJ, Green SJ, Martin NM, Orr AI, et al. Identification and characterization of a novel and specific inhibitor of the ataxia-telangiectasia mutated kinase ATM. *Cancer Res* 2004;64:9152–9.
37. Ziv Y, Jaspers NC, Etkin S, Danieli T, Trakhtenbrot L, Amiel A, et al. Cellular and molecular characteristics of an immortalized ataxia-telangiectasia (group AB) cell line. *Cancer Res* 1989;49:2495–501.
38. Liu Q, Guntuku S, Cui XS, Matsuoka S, Cortez D, Tamai K, et al. Chk1 is an essential kinase that is regulated by Atr and required for the G(2)/M DNA damage checkpoint. *Genes Dev* 2000;14:1448–59.
39. Blasina A, Hallin J, Chen E, Arango ME, Kraynov E, Register J, et al. Breaching the DNA damage checkpoint via PF-00477736, a novel small-molecule inhibitor of checkpoint kinase 1. *Mol Cancer Ther* 2008;7:2394–404.
40. Zhang C, Yan Z, Painter CL, Zhang Q, Chen E, Arango ME, et al. PF-00477736 mediates checkpoint kinase 1 signaling pathway and potentiates docetaxel-induced efficacy in xenografts. *Clin Cancer Res* 2009;15:4630–40.
41. Iacobucci I, Di Rora AG, Falzacappa MV, Agostinelli C, Derenzini E, Ferrari A, et al. *In vitro* and *in vivo* single-agent efficacy of checkpoint kinase inhibition in acute lymphoblastic leukemia. *J Hematol Oncol* 2015;8:125.
42. Faltas BM, Prandi D, Tagawa ST, Molina AM, Nanus DM, Sternberg C, et al. Clonal evolution of chemotherapy-resistant urothelial carcinoma. *Nat Genet* 2016;48:1490–99.
43. Bhagwat AS, Hao W, Townes JP, Lee H, Tang H, Foster PL. Strand-biased cytosine deamination at the replication fork causes cytosine to thymine mutations in *Escherichiacoli*. *Proc Natl Acad Sci U S A* 2016;113:2176–81.
44. Mussil R, Suspene R, Aynaud MM, Gauvrit A, Vartanian JP, Wain-Hobson S. Human APOBEC3A isoforms translocate to the nucleus and induce DNA double strand breaks leading to cell stress and death. *PLoS ONE* 2013;8:e73641.
45. Buisson R, Lawrence MS, Benes CH, Zou L. APOBEC3A and APOBEC3B activities render cancer cells susceptible to ATR inhibition. *Cancer Res* 2017;77:4567–78.
46. Perez RP, Lewis LD, Beelen AP, Olszanski AJ, Johnston N, Rhodes CH, et al. Modulation of cell cycle progression in human tumors: a pharmacokinetic and tumor molecular pharmacodynamic study of cisplatin plus the Chk1 inhibitor UCN-01 (NSC 638850). *Clin Cancer Res* 2006;12:7079–85.
47. Brega N, McArthur GA, Britten C, Wong SG, Wang E, Wilner KD, et al. Phase I clinical trial of gemcitabine (GEM) in combination with PF-00477736 (PF-736), a selective inhibitor of CHK1 kinase. *J Clin Oncol* 2010;28:3062.
48. Manic G, Obrist F, Sistigu A, Vitale I. Trial watch: targeting ATM-CHK2 and ATR-CHK1 pathways for anticancer therapy. *Mol Cell Oncol* 2015;2:e1012976.
49. Kwok M, Davies N, Agathangelou A, Smith E, Oldreive C, Petermann E, et al. ATR inhibition induces synthetic lethality and overcomes chemoresistance in TP53- or ATM-defective chronic lymphocytic leukemia cells. *Blood* 2016;127:582–95.
50. Cottini F, Hideshima T, Suzuki R, Tai YT, Bianchini G, Richardson PG, et al. Synthetic lethal approaches exploiting DNA damage in aggressive myeloma. *Cancer Discov* 2015;5:972–87.
51. Morgado-Palacin I, Day A, Murga M, Lafarga V, Anton ME, Tubbs A, et al. Targeting the kinase activities of ATR and ATM exhibits antitumoral activity in mouse models of MLL-rearranged AML. *Sci Signal* 2016;9:ra91.

# Cancer Research

The Journal of Cancer Research (1916–1930) | The American Journal of Cancer (1931–1940)

## Cytosine Deaminase APOBEC3A Sensitizes Leukemia Cells to Inhibition of the DNA Replication Checkpoint

Abby M. Green, Konstantin Budagyan, Katharina E. Hayer, et al.

*Cancer Res* 2017;77:4579-4588. Published OnlineFirst June 27, 2017.

**Updated version** Access the most recent version of this article at:  
doi:[10.1158/0008-5472.CAN-16-3394](https://doi.org/10.1158/0008-5472.CAN-16-3394)

**Supplementary Material** Access the most recent supplemental material at:  
<http://cancerres.aacrjournals.org/content/suppl/2017/06/27/0008-5472.CAN-16-3394.DC1>

**Cited articles** This article cites 50 articles, 20 of which you can access for free at:  
<http://cancerres.aacrjournals.org/content/77/17/4579.full#ref-list-1>

**Citing articles** This article has been cited by 2 HighWire-hosted articles. Access the articles at:  
<http://cancerres.aacrjournals.org/content/77/17/4579.full#related-urls>

**E-mail alerts** [Sign up to receive free email-alerts](#) related to this article or journal.

**Reprints and Subscriptions** To order reprints of this article or to subscribe to the journal, contact the AACR Publications Department at [pubs@aacr.org](mailto:pubs@aacr.org).

**Permissions** To request permission to re-use all or part of this article, use this link  
<http://cancerres.aacrjournals.org/content/77/17/4579>.  
Click on "Request Permissions" which will take you to the Copyright Clearance Center's (CCC) Rightslink site.